摩擦学学报
TRIBOLOGY

界面润湿性和粗糙度对橡胶滑动摩擦行为的影响

高天燕，张开森，叶家鑫，刘小君，刘焜

Effect of Interface Wettability and Roughness on Sliding Friction Behavior of PDMS

GAO Tianyan, ZHANG Kaisen, YE Jiaxin, LIU Xiaojun, LIU Kun

在线阅读 View online: https://doi.org/10.16078/j.tribology.2022087

DOI: 10.16078/j.tribology.2022087

界面润湿性和粗糙度对橡胶滑动摩擦行为的影响

高天燕, 张开森, 叶家鑫, 刘小君, 刘 焜*
(合肥工业大学 机械工程学院 摩擦学研究所, 安徽 合肥 230000)

摘 要: 当黏弹性体接触界面介于湿和干之间时, 总是捕捉到1个高于干摩擦的润湿状态, 称为黏着态. 该状态下最大摩擦系数称为摩擦峰. 本文中利用涂覆不同材料的载玻片探究了界面润湿性(θ)和粗糙度(Ra)对摩擦峰的影响. 摩擦试验发现, 干燥条件下, Ra相近时, PDMS半球与θ较小的表面, 摩擦更大; θ相近时, 与Ra较小的表面, 摩擦更大. 润湿转变试验中发现, 黏着态下摩擦系数最大增长百分比($\Delta\mu$%)与滞后位移增长百分比(ΔS%)之间呈较好的线性关系. 摩擦系数与滞后位移的增长与接触表面间残余液滴有关. 试验发现: 光滑载玻片表面的Ra相近时, θ较小的表面, 摩擦峰较低; θ相近时, Ra较小的表面, 摩擦峰较低. 该结果表明, 黏着态下接触区域内微液桥的数量和形状对摩擦峰具有重要影响.

关键词: 摩擦峰; 黏着态; PDMS半球; 接触角; 表面粗糙度
中图分类号: TH117.1 **文献标志码:** A **文章编号:** 1004-0595(2023)07–0750–08

Effect of Interface Wettability and Roughness on Sliding Friction Behavior of PDMS

GAO Tianyan, ZHANG Kaisen, YE Jiaxin, LIU Xiaojun, LIU Kun*

(*Institute of Tribology, School of Mechanical Engineering, Hefei University of Technology, Anhui Hefei 230000, China*)

Abstract: When the contact interface of visco-elastomers is between wet and dry, a new wetting condition higher than the dry friction is always captured, which is called the tacky regime. The maximum friction coefficient in this state is termed as the friction peak. In this manuscript, the influences of wettability (θ) and surface roughness (Ra) of glass slide surfaces on the friction peak were investigated using a custom-built in-situ optical microtribometer. Different glass slides were chosen as the base including transparent glass slide, teflon (PTFE) tape + glass slide and polypropylene (BOPP) + glass slide, which named as sample A, B and C, respectively. The contact angles of sample A, B and C were 38°, 97° and 100°, and the surface roughness of sample A, B and C were 1.420 μm, 1.315 μm and 0.312 μm, respectively. As the soft surface, a PDMS hemesphere with the ratio of the curing agent to the base of 1:5 was produced under water on a glass plate. The diameter of the resulting PDMS sphere was 3.58 mm with the contact angle of 110°. Two kinds of sliding experiments were conducted between the three samples and the PDMS hemisphere including dry condition and wet to dry condition. It was found that in the dry condition when the surface roughnesses of the glass slide were similar, the friction between the PDMS hemisphere and the surface with the smaller contact angle was larger; when the contact angles of the glass slide surfaces were similar, the friction of the surface with the smaller surface roughness was larger. In the friction experiments where the contact interface changed from wet to dry, the maximum friction coefficients of the sample A, B and C were 1.20, 1.02 and 1.25, respectively. In order to compare the tribological behaviors of the three samples in the tacky regime, the increased percentage of the maximum friction coefficient compared with the dry friction

Received 10 May 2022, revised 12 July 2022, accepted 12 July 2022, available online 1 August 2023.
*Corresponding author. E-mail: liukun@hfut.edu.cn, Tel: +86-551-62901756-2729.
This project was supported by the National Natural Science Foundation of China (51875153, 51875152, 51975174).
国家自然科学基金(51875153, 51875152, 51975174)资助.

coefficient was defined as the relative increased percentage, $\Delta\mu$%, and the increased percentage of hysteresis displacement in the tacky regime compared with the dry condition was defined as ΔS%. The result showed that the $\Delta\mu$% of the three samples were 15%, 70%, 28% and ΔS% of the three samples were 20%, 130%, 40%. It was found that there was a good linear relationship between the maximum increase percentage of friction coefficient ($\Delta\mu$%) and the increase percentage of hysteresis displacement (ΔS%) comparing with those in the dry condition. The increase of friction coefficient and hysteresis displacement might be related to the residual droplets between the contact surfaces. It was conjectured that the wettability and surface roughness of the glass slide surfaces would affect the shape and number of liquid bridge generated in the contact interfaces, thus affecting the increase of the friction peak in the tacky regime. When the surface roughness of the smooth glass slide surface was similar, the friction peak of the surface with smaller contact angle was lower. In this condition, the hydrophilic surface was more unfavorable to the formation of liquid bridge between the asperities, thus reduced the maximum friction peak. When the contact angle was close, the friction peak of the surface with smaller surface roughness was lower. We hypothesis that for the smoother glass slide surface, the real contact area with the PDMS hemisphere was larger, which promoted dewetting of water film in the contact interfaces, resulting in the reduction of capillary adhesion in the tacky regime, and thus weakened the friction peak. For smooth hydrophobic surfaces, micro-scale roughness might promote the friction peak in the tacky regime. We proposed that the friction peak in the tacky regime might be affected by the interface dewetting behavior, the number and the shape of the micro-liquid bridges in the sliding process, and the specific mechanism needed to be studied and discussed further.

Key words: friction peak; tacky regime; PDMS hemisphere; contact angle; surface roughness

橡胶作为1种典型的黏弹性体材料，被广泛应用于车辆轮胎[1,2]、雨刮器[3-4]、密封圈[5]及鞋底[6]等领域. 橡胶的摩擦和磨损一直是摩擦学领域重要的研究内容之一[7]. 下雨后，雨刮器在滑动中往往会出现噪音及运动不平稳的现象[8]. Deleau等[3]和Gao等[9–12]通过试验发现黏弹性体接触界面由湿到干期间往往会出现1个高于干摩擦的润湿状态，并称之为黏着态. 这种黏着态下的高摩擦响应会加剧橡胶配件的磨损，缩短其使用寿命，其磨损产生的微纳米尺度的碎屑会加剧环境污染，甚至危害人类的呼吸健康. 相反，如果对这种黏着态现象加以利用，实现雨天刹车距离的缩短以及鞋底抓地力的提高，对于降低车辆事故和滑倒事故的风险具有重要意义.

黏着态下，接触区域残余液体及分子间相互作用对于摩擦的增长具有重要影响. Gao等[10]探究了水膜占比对润湿转变过程中摩擦的影响，发现黏着态摩擦峰与高剪切强度的水膜有关. 类似地，许多昆虫可以在天花板和垂直表面平稳爬行，这一能力被归结于粗糙度、液体分泌(毛细和黏度效应)和范德华相互作用[13-14]. 研究发现，昆虫衬垫的内部纤维可能对附着力的增加具有重要作用，并且其分泌的黏性液体通过提高毛细和黏性黏附可以补偿小尺度粗糙度带来的真实接触面积的损失[15–18]. 关于润湿性对昆虫黏附力的影响，Voigt等[19]指出疏水性的基底表面更有利于附着. 本文中作者利用自主搭建的原位观测摩擦试验台探究了涂覆不同材料的载玻片与硅橡胶接触界面由湿到干过程摩擦系数的演变规律，分析了不同载玻片表面特性对黏着态下摩擦峰的影响.

1　试验部分

1.1　试验装置

如图1结构图所示，微牛级原位观测摩擦试验台由运动系统、力测量系统和光学观测系统3部分组成. 运动系统利用伺服电机(MDI, IMS, USA)通过联轴器和丝杠实现线性往复运动. 力测量系统选用平行四边形软悬臂梁结构和电容式位移传感器(D-510.020, PI, Germany). 摩擦试验中，利用水平和竖直2个方向的位移传感器分别测量悬臂梁在竖直和水平方向的位移偏转量. 然后，根据杆的纯弯曲理论[20]，可以实现从位移偏转量到力的转换. 该试验装置中选用的软悬臂梁的力测量精度为±14 μN. 光学观测系统是1台倒置的金相显微镜(MR3000)，并配备有20×物镜. 另外，显微镜的光路中安装了滤波片(中心波长589.3 ±10 nm)，并且还外配了1台数码相机(分辨率：0.6 piexl/μm；拍摄速率：7 frame/s).

摩擦试验中，上试样选用聚二甲基硅氧烷(PDMS)半球并通过尼龙杆件固定在L型板上. 下试样选用3种载玻片(尺寸：76 cm×26 cm×1 mm)：普通载玻片、粘贴有聚四氟乙烯(PTFE)薄膜的载玻片和粘贴有聚丙烯(BOPP)薄膜的载玻片(分别命名为样本A、B和C)，并固定于水平位移台上. 为了试验操作方便以及实现对接触区域的观测，下试样均选择载玻片作为基底. 在

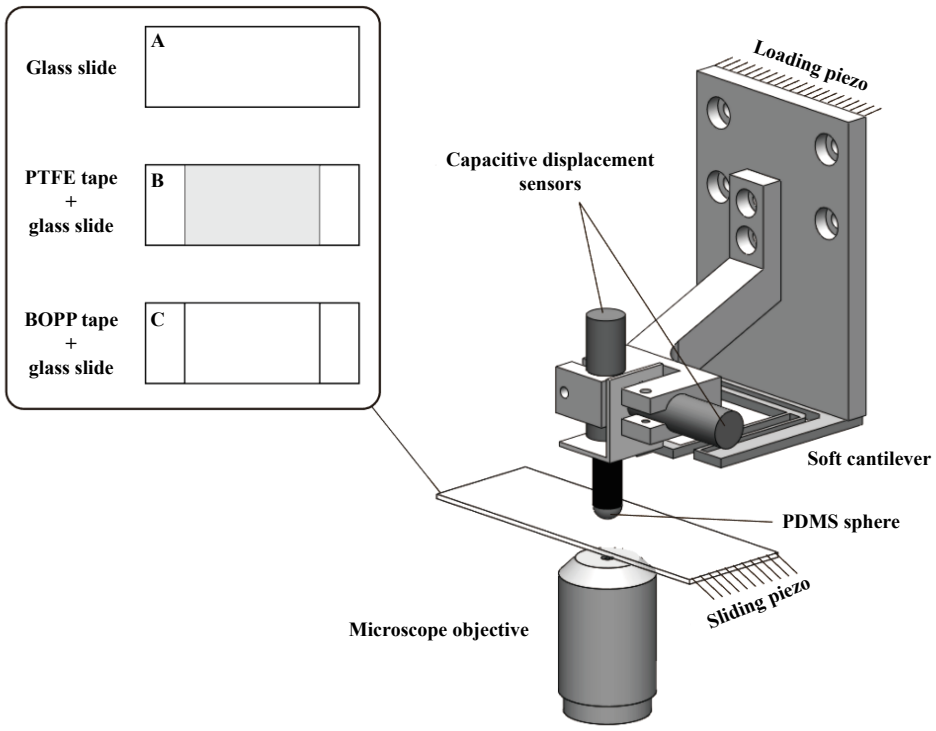

Fig. 1 Schematic diagram of in-situ optical micro tribometer

图 1 微牛级原位观测摩擦试验台原理图

施加载荷之前，首先在下试样表面滴加0.3 μL的去离子水，然后将PDMS半球与下表面接触并在外载荷为3 mN的作用下进行线性往复运动(滑动速度：20 μm/s，行程：200 μm)，同时记录接触界面润湿转变过程(从湿到干)中摩擦系数的演变过程. 另外，空白对照组中接触区域没有滴加去离子水，即干燥条件. 所有摩擦试验开展的环境条件为室温25 ℃、湿度30%~40%.

1.2 试验材料及制备

如图2所示，PDMS半球的制备，首先是将预聚体(组分A)与固化剂(组分B)按照质量比5:1进行搅拌混合，然后将混合物放置在真空泵中进行脱气约20 min，直到没有气泡产生[20-21]. 另外，制备中选择玻璃板作为基片，制备前，先将基片依次放置在丙酮和去离子水溶液中用超声清洗器超声振荡10 min，并将清洗后的玻璃板放置在装有水溶液的培养皿中. 然后利用注射器将脱气后的PDMS混合物转移到该培养皿中的玻璃板上，PDMS混合物在水下由于表面张力的作用而呈现球状[22]. 然后将培养皿常温下静置24 h后，把玻璃板从水中取出置于鼓风干燥箱中，在80 ℃条件下加热90 min，得到的PDMS半球的直径为3.58 mm，弹性模量约为3 MPa. 利用光学接触角测量仪(SL200KS，KINO，USA)测得PDMS半球的润湿接触角约为115°，并利用三维共聚焦显微镜(VK-X250，Keyence，Japan)测得其表面粗糙度，约为120±3 nm.

2 结果与讨论

2.1 不同载玻片表面的材料特性

为了确定3种载玻片样本的表面润湿性，利用光学接触角测量仪测量了固-液接触角(θ). 试验中选择去离子水作为测量液体，每次试验滴加的液体体积为2 μL. 然后利用ImageJ软件对润湿图片(图3)进行处理分析，得到接触角. 每个样本的润湿接触角由5组测量数据的平均值得到. 图3中展示了样本A、B和C的润湿图片以及接触角的测量结果. 从试验结果中可以看出样本A为亲水性表面(θ<90°)，样本B和C为疏水表面(θ>90°)，并且润湿接触角相近.

3种载玻片样本的表面形貌通过三维共聚焦显微镜测得，试验选取20×镜头进行观测. 算数平均粗糙度(Ra)计算中，测量区域为200 μm×200 μm，每种载玻片样本测量5次，每种载玻片样本的Ra都是由5组测试结果的均值得到. 图4所示为样本A、B和C的表面形貌照片及Ra的测量结果. 测量结果显示，样本A和B的Ra相近且约为样本C的4倍，表明样本A和B的表面比样本C更粗糙.

2.2 PDMS半球在不同载玻片表面的滑动摩擦过程分析

图5所示为干燥条件下，PDMS半球在3种载玻片表面的动态摩擦系数. 图5(a)所示为1个试验周期内摩

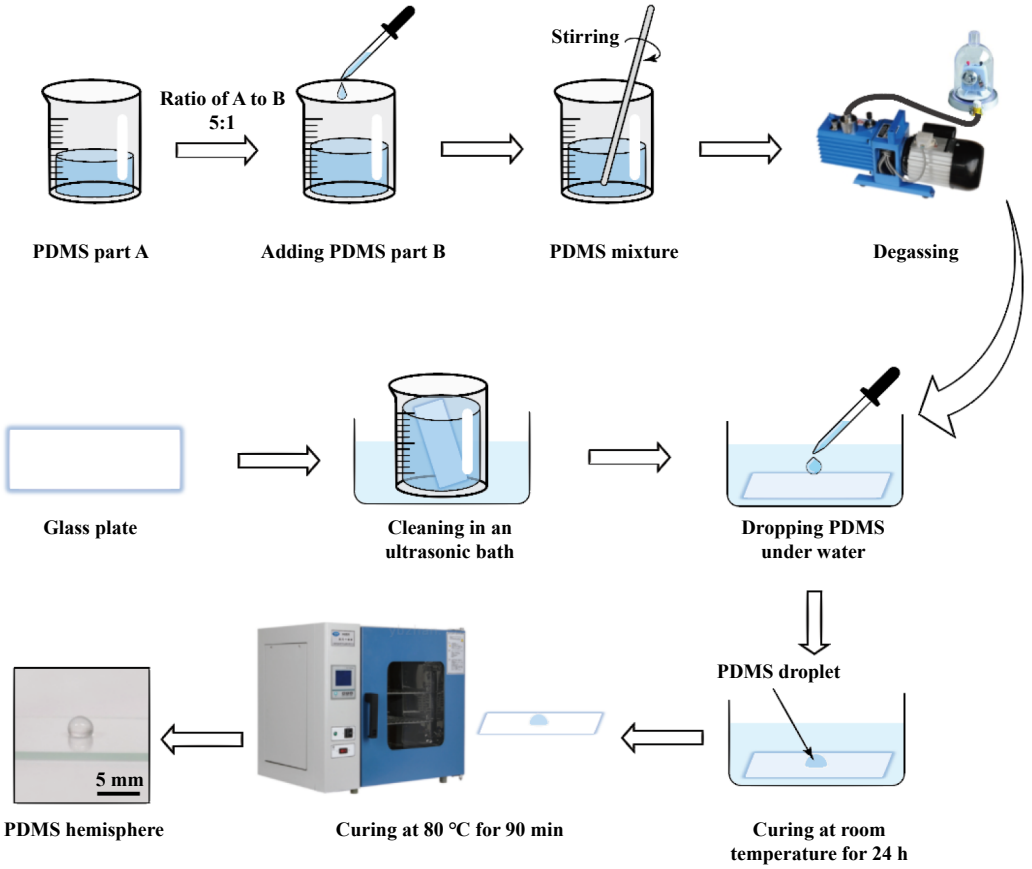

Fig. 2　Diagram of preparation process of PDMS hemisphere

图 2　PDMS半球的制备流程图

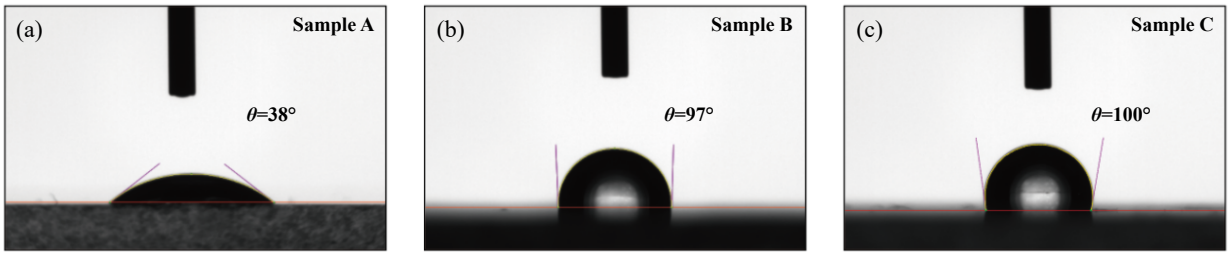

Fig. 3　Measurement results of contact angle: (a) sample A; (b) sample B; (c) sample C

图 3　润湿接触角的测量结果: (a) 样本A; (b) 样本B; (c) 样本C

擦系数随位移的变化规律. 可以看出, 在滑动方向发生转变时, 摩擦系数随着位移的变化而呈现出滞后特性. 为了表征单个周期的橡胶摩擦系数, 选择图5(a)中的黑色虚线框作为原始计算数据. 通过将正、反2个方向的数据点取平均值[23-24], 可以消除安装倾斜带来的测量误差, 得到单个周期的摩擦系数.

$$\mu = \frac{\mu_{\mathrm{f}} - \mu_{\mathrm{r}}}{2} \tag{1}$$

其中, μ_{f}表示前进方向的摩擦系数, μ_{r}表示后退方向的摩擦系数. 3种样本的干摩擦系数均通过该计算方法得到, 如图5(b)所示. 样本A、B和C的干摩擦系数分为1.05、0.60和0.98.

不同于其他材料摩擦, 橡胶摩擦主要由黏着项和滞后项2部分组成[25-26]. 当发生相对滑动的表面较为光滑时, 摩擦阻力主要来源于黏着摩擦. 黏着摩擦与真实接触面积和表面自由能有关, 橡胶摩擦系数随着表面自由能的增加而增大[7, 27]. 样本A和B的表面粗糙度相近, 并且样本A为亲水性表面, 样本B为疏水性表面. 样本A的干摩擦系数高于样本B, 这一结果应该与样本A的高表面能有关. 样本B和C的润湿接触角相近, 样本B的表面粗糙度约是样本C的4倍, 摩擦试验发现样本C的干摩擦系数比样本B的大. 这一结果与粗糙度

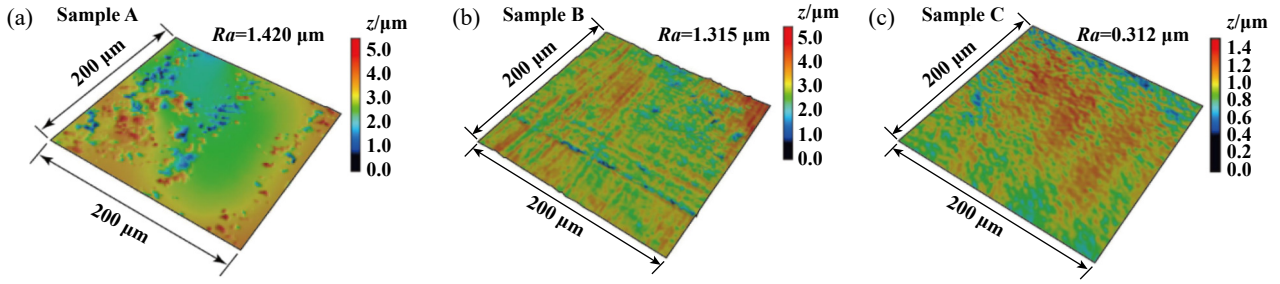

Fig. 4 Measurement results of three-dimensional surface roughness: (a) sample A; (b) sample B; (c) sample C

图 4 三维表面粗糙度的测量结果：(a) 样本A；(b) 样本B；(c) 样本C

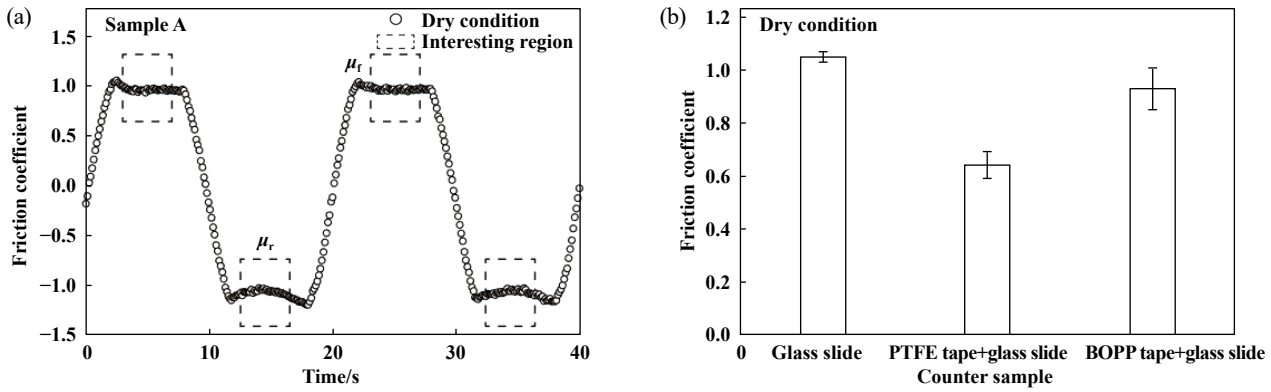

Fig. 5 (a) Dry friction coefficient between PDMS hemisphere and glass slide sample A; (b) measurement results of dry friction coefficient of three glass slide samples

图 5 (a) PDMS半球与载玻片样本A的滑动干摩擦系数随时间的变化过程；(b) 3种载玻片样本干摩擦系数的测量结果

的引入会降低橡胶摩擦的理论相一致，粗糙度的引入使得真实接触面积减小，从而削弱黏着项的贡献[26].

摩擦试验探究了PDMS半球与样本A、B和C接触界面由湿到干过程中滑动摩擦系数的演变规律. 根据图5(a)所展示的摩擦系数处理方法，得到了润湿转变过程中摩擦系数随时间的变化过程，如图6(a~c)所示. 图6(a~c)中的由蓝到白的渐变过程代表了接触区域间水逐渐挥发的过程，白色代表接触区域干燥条件下的摩擦状态. 可以看出，样本A、B和C的摩擦系数随时间的演变规律基本相同，动态滑动初期，摩擦系数均是先基本保持不变(分别为0.84、0.54和1.12)，然后减小到1个极小值(分别为0.79、0.43和1.03)，随着时间的推移，水进一步挥发，摩擦系数又逐渐增大到1个最大值(分别为1.20、1.02和1.25). 从摩擦系数随时间的变化图可以看出，样本A、B和C在接触区域由湿到干的过程中均出现1个高于干摩擦系数的峰值，该峰值称为摩擦峰，用μ_{peak}表示，摩擦峰相比于干摩擦系数μ_{dry}的增长称为相对增长百分比，用$\Delta\mu$%表示，$\Delta\mu\%=(\mu_{peak}-\mu_{dry})/\mu_{dry}\times100\%$. 图6(d)所示为样本A、B和C相对增长百分比的结果，该结果分别由3组试验得到. 结果表明，样本A和样本C的$\Delta\mu$%较低，分别为15%和28%，样本B的$\Delta\mu$%相对较高，高达约70%.

图7(a~c)所示为1个运动周期内，样本A、B和C在干燥(白色数据点)和黏着态(灰色数据点)条件下的摩擦系数随位移的变化过程. 图7(a~c)的试验结果显示，当PDMS半球的运动方向发生改变时，摩擦系数随位移的改变呈现出明显的滞后特性. 可以看出，相比于干燥条件，样本A、B和C在黏着态下摩擦系数均表现出更明显的滞后效应. 为了量化样本A、B和C在干燥和黏着态条件下的滞后特性，将从运动方向改变到摩擦系数减小为0的位移定义为滞后位移，用ΔS表示. 图7(d)所示为样本A、B和C在干燥和黏着态条件下滞后位移结果. 由图7(d)可以看出，样本A、B和C在干燥条件下的滞后位移用ΔS_{dry}表示，其值分别为36、16和27 μm，在黏着态条件下的滞后位移用ΔS_{tacky}表示，其值分别为44、38和39 μm. 通过计算发现，样本B在黏着态下的ΔS_{tacky}相比于干燥条件的ΔS_{dry}增长百分比$\left(\Delta S\% = \dfrac{\Delta S_{tacky}-\Delta S_{dry}}{\Delta S_{dry}}\times100\%\right)$最大，约为130%.

根据上述试验结果，可以计算得到样本A、B和C的$\Delta\mu$%分别为15%、70%和28%以及ΔS%分别为20%、130%和40%. 为了分析$\Delta\mu$%与ΔS%相关性，绘制了$\Delta\mu$%与ΔS%散点图，如图8所示. 由图8可以看出，$\Delta\mu$%

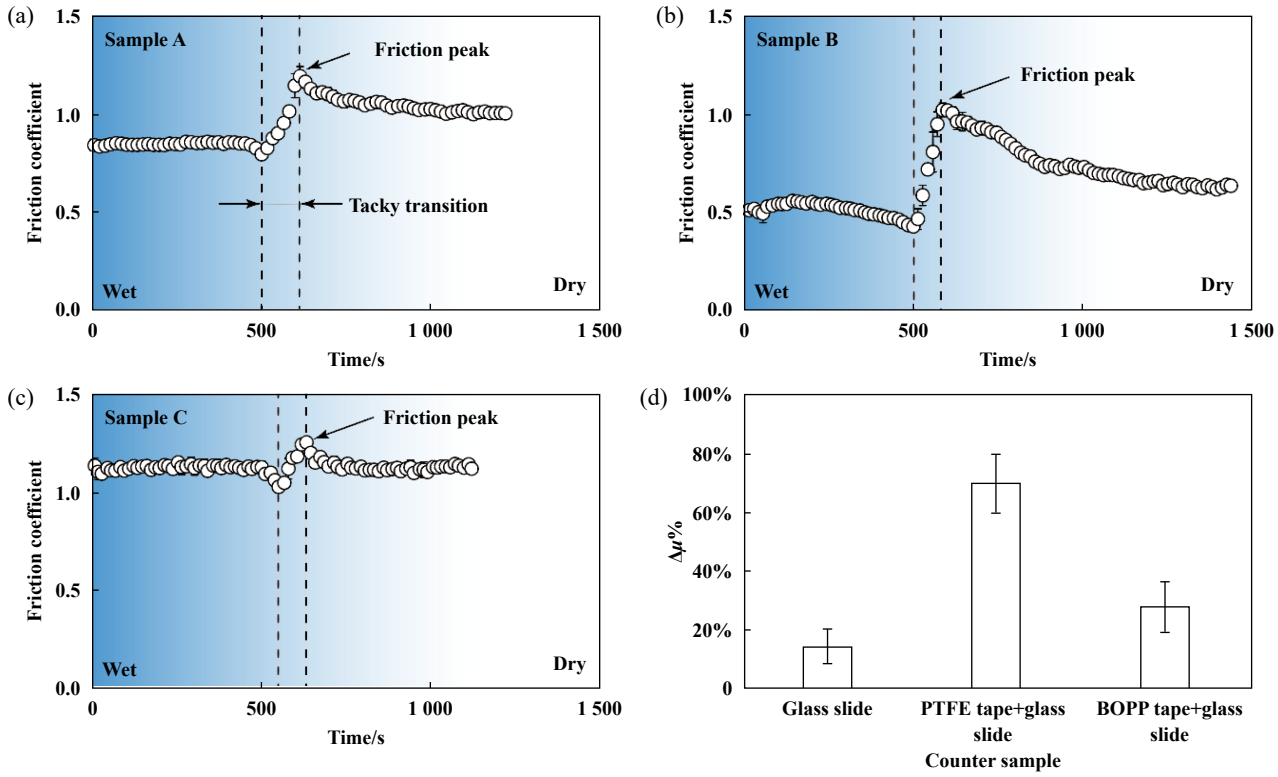

Fig. 6　Evolution of friction coefficient during the wetting transition between PDMS hemisphere and glass slide samples: (a) sample A; (b) sample B; (c) sample C; (d) measurement results of the relative percentage increase of friction peak of the three glass slide samples

图 6　PDMS半球与3种载玻片样本接触界面润湿转变过程中摩擦系数的演变过程: (a) 样本A; (b) 样本B; (c) 样本C; (d) 3种载玻片样本中摩擦峰的相对增长百分比的测量结果

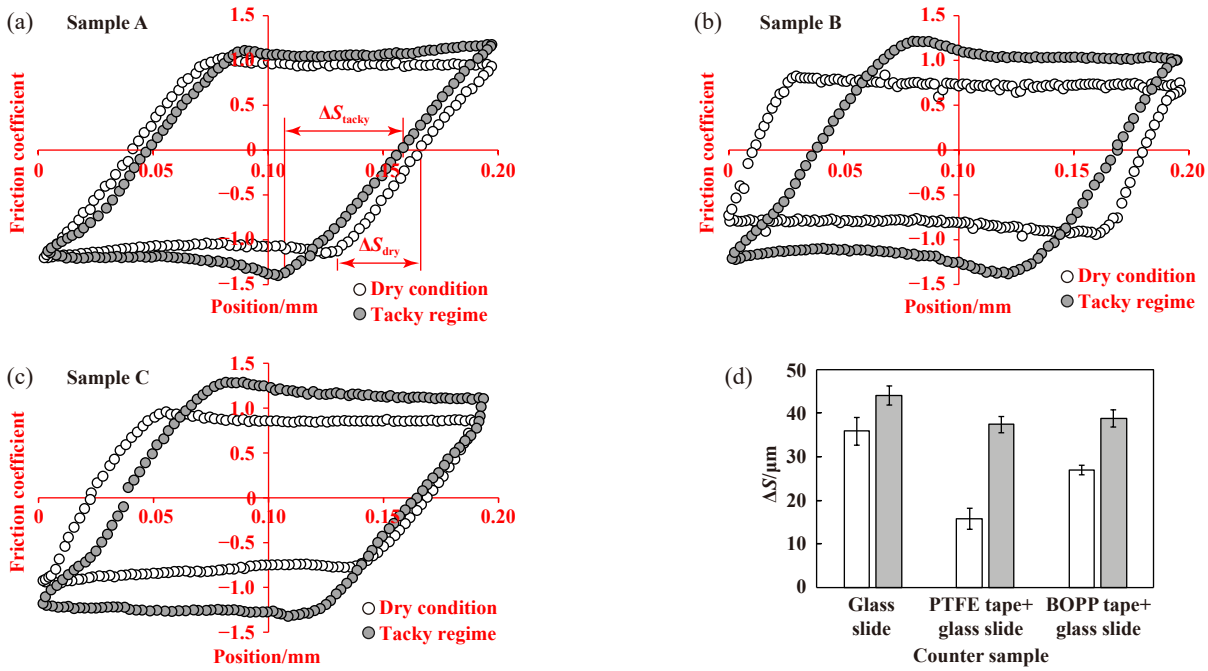

Fig. 7　Evolution of friction coefficient with displacement under dry and tacky conditions: (a) sample A; (b) sample B; (c) sample C; (d) measurement results of lag displacement of the three slide samples under dry and tacky conditions

图 7　干燥和黏着态条件下摩擦系数随位移的演变规律: (a) 样本A; (b) 样本B; (c) 样本C; (d) 3种载玻片样本在干燥和黏着态条件下滞后位移的测量结果

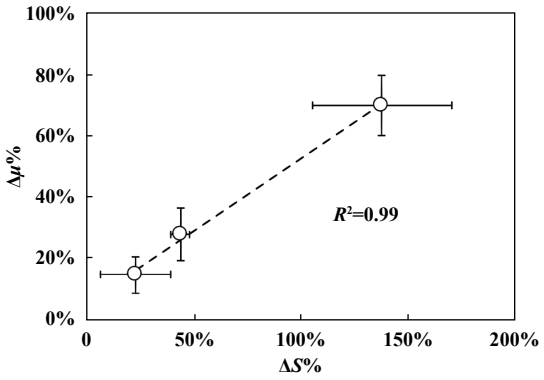

Fig. 8 Linear correlation between the increase percentages of friction coefficient ($\Delta\mu$%) and lag displacement (ΔS%)

图 8 摩擦系数增长百分比($\Delta\mu$%)与滞后位移增长百分比(ΔS%)之间的线性相关性

随ΔS%的增大而增大，通过线性拟合发现$\Delta\mu$%与ΔS%呈现出较好的线性相关性，其中相关系数R^2为0.99. 该结果表明，摩擦系数在位移上的滞后特性与摩擦峰的增长呈线性相关.

2.3 摩擦峰与表面粗糙度和润湿性的关联性分析

橡胶摩擦在位移上的滞后特性，从根本上讲，与接触面的表面特性(如黏附能、表面自由能、润湿性及表面粗糙度等)有关[7, 27]. Gao等[9]通过静态接触试验发现润湿转变过程中法向载荷先减小后增大，并指出接触界面毛细黏附作用对摩擦峰的出现具有重要影响. 通过分析接触区域水膜占比与摩擦系数的关系，Gao等[10]指出黏着过渡期间接触区高剪切强度水膜是摩擦系数增长的主要原因. 并且通过计算接触区域离散液膜的厚度分布，在之前发表的文章中作者提出黏着态摩擦的增长与接触区域内离散分布的液桥有关[12]. 根据样本A、B和C的润湿接触角和表面粗糙度以及摩擦试验结果，推测样本B与PDMS半球之间的表面微凸体在黏着状态下更容易形成微液桥，其在滑动过程中的剪切阻力是摩擦增加的重要因素. 图9所示为黏着状态下样本A、B和C接触区残余水滴的分布示意图. 从图9中可以看出，对于Ra相近的样本A和B，由于样本A的润湿接触角较小，所以，相同体积的水滴在样本A表面的高度更低，更不利于接触区域内微液桥的形成. 对于均为疏水表面且润湿接触角相近的样本B和C，Ra更小的样本C (约为样本B的1/4)在润湿转变中却出现了$\Delta\mu$%更小的现象. 这一试验结果与现实生活中的现象相反，比如粗糙度的引入会使黏附降低. 猜想这是因为，相比于样本B，样本C表面的粗糙度更小，所以与PDMS半球的真实接触区域占比更大，从而更有利于接触区域内水膜的排出，使得黏着态下样本C接触区域残余的液滴更少，导致毛细黏附力降低，从而削弱摩擦的增长. 对于光滑的疏水表面，微米级粗糙度的引入可能对黏着态摩擦峰具有促进作用. 滑动过程中界面的去湿行为、微液桥数量和形状等都可能对摩擦峰产生影响，具体的作用机理还需要作进一步的研究与探讨.

3 结论

a. 表面粗糙度相近时，表面润湿性较强的表面与PDMS半球的干摩擦较大；表面润湿性相近时，表面粗糙度较低的表面与PDMS半球的干摩擦较大.

b. 黏弹性体接触界面由湿到干过程中，总是观察到1个高于干摩擦系数的润湿状态，称为黏着态. 润湿转变过程中，摩擦系数先基本不变，然后减小到1个极小值后开始增大，增大到某个最大值后，然后减小最终趋于稳定. 相比于干燥条件，黏着态下的PDMS半球的滞后位移增大. $\Delta\mu$%与ΔS%之间存在较好的线性关系，$\Delta\mu$%随着ΔS%的增大而增大.

c. 不同载玻片表面的润湿性和粗糙度都会影响摩擦峰的增长幅度. 而表面的润湿性和粗糙度关系到接触表面之间液桥的数量和形状，从而影响黏着态下摩擦峰的增长幅度. 载玻片表面粗糙度相近时，较亲水的表面更不利于微凸体之间液桥的形成，从而削弱摩擦峰的增长幅度；载玻片表面疏水性相近时，微米级粗糙度的引入可以促进摩擦峰的增长幅度.

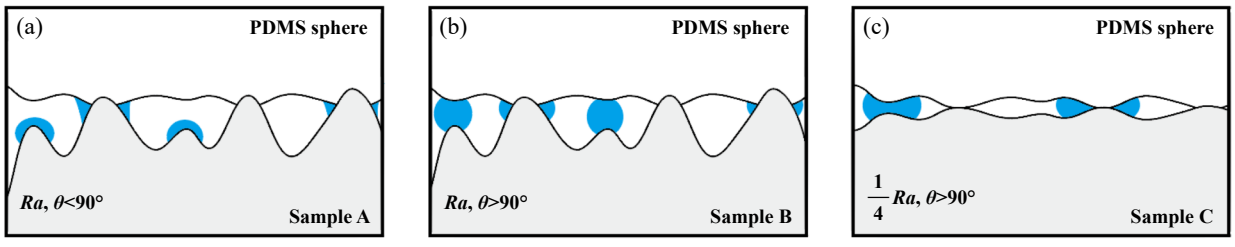

Fig. 9 Distribution illustration of residual water droplets in the contact region under tacky regime: (a) sample A; (b) sample B; (c) sample C

图 9 黏着状态下接触区残余水滴的分布示意图: (a) 样本A; (b) 样本B; (c) 样本C

参考文献

[1] Yang Yiyang. Study of tread rubber friction mechanism and tire cornering properties under complex conditions[D]. Changchun: Jilin University, 2016 (in Chinese) [杨一洋. 胎面橡胶摩擦机理及复杂工况下轮胎侧偏特性研究[D]. 长春: 吉林大学, 2016].

[2] Heinrich G, Klüppel M. Rubber friction, tread deformation and tire traction[J].Wear,2008,265(7-8):1052–1060.doi:10.1016/j.wear.2008.02.016.

[3] Deleau F, Mazuyer D, Koenen A. Sliding friction at elastomer/glass contact: influence of the wetting conditions and instability analysis[J]. Tribology International, 2009, 42(1): 149–159. doi: 10.1016/j.triboint.2008.04.012.

[4] Wagner P, Wriggers P, Klapproth C, et al. Multiscale FEM approach for hysteresis friction of rubber on rough surfaces[J]. Computer Methods in Applied Mechanics and Engineering, 2015, 296: 150–168. doi: 10.1016/j.cma.2015.08.003.

[5] Tan Guibin, Fan Qing, Tan Feng, et al. Advances in tribology on elastomer sealing and its future trends for the huge machinery[J]. Tribology, 2016, 36(5): 659–666 (in Chinese) [谭桂斌, 范清, 谭锋, 等. 重大装备橡塑密封系统摩擦学进展与发展趋势[J]. 摩擦学学报, 2016, 36(5): 659–666]. doi: 10.16078/j.tribology.2016.05.018.

[6] Nishi T, Yamaguchi T, Shibata K, et al. Friction behavior of silicone rubber hemisphere under non-uniform wetting states: with water droplets in air or air bubbles in water[J]. Tribology International, 2021, 155: 106769. doi: 10.1016/j.triboint.2020.106769.

[7] Persson B N J. On the theory of rubber friction[J]. Surface Science, 1998, 401(3): 445–454. doi: 10.1016/S0039-6028(98)00051-X.

[8] de Gennes P-G, Brochard-Wyart F, Quere D. Capillarity and wetting phenomena: drops, bubbles, pearls, waves[M]. New York: Springer, 2013.

[9] Gao, Tianyan, Ye Jiaxin, Zhang Kaisen, et al. Role of capillary adhesion in the friction peak during the tacky transition[J]. Friction, 2021, 10(8): 1208-1216. doi: 10.1007/s40544-021-0524-2.

[10] Gao Tianyan, Liu Kun, Zhang Kaisen, et al. Transient high friction dominated by high shear strength residual water film[J]. Tribology Letters, 2022, 70(1): 29. doi: 10.1007/s11249-022-01569-4.

[11] Gao Tianyan, Zhang Kaisen, Ye Jiaxin, et al. Effect of PDMS material properties and sliding velocity on friction peak in tacky regime[J]. Tribology, 2023, 43(6): 597-605 (in Chinese) [高天燕, 张开森, 叶家鑫, 等. PDMS材料特性和滑动速度对黏着态下摩擦峰的影响[J]. 摩擦学学报, 2023, 43(6): 597-605]. doi: 10.16078/j.tribology. 2022041.

[12] Gao Tianyan, Zhang Kaisen, Liu Xiaojun, et al. Linking macroscale frictional properties to nanoscale water capillary bridges[J]. Tribology International, 2022, 174: 107696. doi: 10.1016/j.triboint.2022.107696.

[13] Gao Huajian, Wang Xiang, Yao Haimin, et al. Mechanics of hierarchical adhesion structures of geckos[J]. Mechanics of Materials, 2005, 37(2–3): 275–285. doi: 10.1016/j.mechmat.2004.03.008.

[14] Zhang Hao, Guo Dongjie, Dai Zhendong. Progress on gecko-inspired micro/nano-adhesion arrays[J]. Chinese Science Bulletin, 2010, 55(18): 1843–1850. doi: 10.1007/s11434-010-3065-z.

[15] Zhou Yanmin, Robinson A, Steiner U, et al. Insect adhesion on rough surfaces: analysis of adhesive contact of smooth and hairy pads on transparent microstructured substrates[J]. Journal of the Royal Society Interface, 2014, 11(98): 20140499. doi: 10.1098/rsif.2014.0499.

[16] Bowden F P, Tabor D. The friction and lubrication of solids[M]. New York: Oxford University Press, 2001.

[17] Kwak J S, Kim T W. A review of adhesion and friction models for gecko feet[J]. International Journal of Precision Engineering and Manufacturing, 2010, 11(1): 171–186. doi: 10.1007/s12541-010-0020-5.

[18] Samoilov V N, Sivebaek I M, Persson B N J. The effect of surface roughness on the adhesion of solid surfaces for systems with and without liquid lubricant[J]. The Journal of Chemical Physics, 2004, 121(19): 9639–9647. doi: 10.1063/1.1806814.

[19] Voigt D, Perez Goodwyn P, Sudo M, et al. Gripping ease in southern green stink bugs Nezara viridula L. (Heteroptera: Pentatomidae): coping with geometry, orientation and surface wettability of substrate[J]. Entomological Science, 2019, 22(1): 105–118. doi: 10.1111/ens.12345.

[20] Dong Conghui, Zhang Yafeng, Tang Cheng, et al. Dynamic frictional behavior of microdroplets on PDMS soft substrate[J]. Tribology, 2021, 41(5): 619–626 (in Chinese) [董聪慧, 张亚锋, 汤程, 等. 微液滴在PDMS软基体表面的动态摩擦行为研究[J]. 摩擦学学报, 2021, 41(5): 619–626]. doi: 10.16078/j.tribology.2020137.

[21] Maegawa S, Nakano K. Dynamic behaviors of contact surfaces in the sliding friction of a soft material[J]. Journal of Advanced Mechanical Design, Systems, and Manufacturing, 2007, 1(4): 553–561. doi: 10.1299/jamdsm.1.553.

[22] Nanjundiah K, Hsu P Y, Dhinojwala A. Understanding rubber friction in the presence of water using sum-frequency generation spectroscopy[J]. The Journal of Chemical Physics, 2009, 130(2): 024702. doi: 10.1063/1.3049582.

[23] Burris D L, Sawyer W G. Addressing practical challenges of low friction coefficient measurements[J]. Tribology Letters, 2009, 35(1): 17–23. doi: 10.1007/s11249-009-9438-2.

[24] Schmitz T L, Action J E, Burris D L, et al. Wear-rate uncertainty analysis[J]. Journal of Tribology, 2004, 126(4): 802–808. doi: 10.1115/1.1792675.

[25] Cao Ping, Yan Xinping, Bai Xiuqin. Theory analyses of effect of topography on skid resistance of asphalt pavements[J]. Tribology, 2009, 29(4): 306–310 (in Chinese) [曹平, 严新平, 白秀琴. 沥青路面形貌对抗滑性能影响的理论分析[J]. 摩擦学学报, 2009, 29(4): 306–310]. doi: 10.3321/j.issn:1004-0595.2009.04.003.

[26] Persson B N J, Albohr O, Tartaglino U, et al. On the nature of surface roughness with application to contact mechanics, sealing, rubber friction and adhesion[J]. Journal of Physics: Condensed Matter, 2005, 17(1): R1–R62. doi: 10.1088/0953-8984/17/1/R01.

[27] Mori K, Kaneda S, Kanae K, et al. Influence on friction force of adhesion force between vulcanizates and sliders[J]. Rubber Chemistry and Technology, 1994, 67(5): 797–805. doi: 10.5254/1.3538711.